10.3 A REAL-TIME TURBULENCE MODEL (RTTM) DESIGNED FOR THE OPERATIONAL PREDICTION OF AVIATION TURBULENCE ENVIRONMENTS

M. L. Kaplan, J. J. Charney**, K. T. Waight III*, Y.-L. Lin, K. M. Lux, A. W. Huffman, and J. D. Cetola
Department of Marine, Earth, and Atmospheric Sciences
North Carolina State University
Raleigh, North Carolina 27695-8208
*MESO Inc.
1005 Capability Drive
Raleigh, North Carolina 27695-8208
**Current Affiliation: USDA/Forest Service, North Central Research Station, East Lansing, MI 48823

1. INTRODUCTION

We will describe the numerical modeling system and postprocessor employed in the Real-Time Turbulence Model (RTTM) run operationally at North Carolina State University in support of NASA's B-757 turbulence research missions. We will focus on a description of the key turbulence forecasting index in this system based on a paradigm developed by Kaplan et al. 2002. Additionally, this paper will focus on a real-time example of the model, its index, and simulated precipitation and wind fields associated with case studies of observed turbulence as reported by commercial aircraft. The ability of the model to isolate, in real time, regions of significant turbulence potential will be explored, in particular, compared with the NCAR RAP ITFA forecast index.

2. THE NUMERICAL MODEL AND POSTPROCESSOR

The numerical model is MASS version 5.13 (Kaplan et al. 2002). The MASS model is a hydrostatic terrain-following sigma coordinate system with comprehensive boundary layer and convective parameterizations. The model is integrated over three different horizontal resolutions, i.e., 60 km, 30 km, and 15 km for the coarse, fine1, and fine2 grids with the finest two meshes employing one-way nested-grid lateral boundary conditions. The grid matrix size is 70X60X50 points for the 60 km mesh and 90x100x50 for the 30 km and 15 km meshes. The sigma-p surfaces are spaced such that the vertical separation is about 20 mb between 850 and 400 mb with wider spacing above. There are also 15 levels below 850 mb to ensure proper convective triggering. The initial state for the coarse mesh is provided by the NWS ETA 80 km analyses at 0000 UTC and 1200 UTC as well as reanalyzed rawinsonde and aviation surface observations analyzed with an optimum interpolation scheme. Time-dependent lateral boundary conditions are derived from the NWS ETA 40 km forecast model and are updated every 3 hours. The ETA input is actually on an 80 km grid because of the way NCEP archives it. Hourly coarser mesh simulated fields serve as the time-dependent lateral boundary conditions for the 30 and 15 km grid meshes. The 30 km simulation is initialized at 0300 UTC and 1500 UTC from the coarse mesh simulation and the 15 km simulation is initialized at 0600 UTC and 1800 UTC from the fine1 simulation. The three grids are located in a manner that allows them to be integrated over the entire 24-hour period, i.e., 24 hours at the coarse mesh, 21 hours at the fine1 mesh, and 18 hours at the fine2 mesh. They are integrated from the NWS ETA analysis data cycles consistent with the range of typical operational NASA-Langley B-757 turbulence research flights. The modeling system is designed solely to support the NASA turbulence research flight missions.

The postprocessing system is designed to support real-time forecasts of turbulence potential for use in directing the NASA B-757 research aircraft to locations of turbulence. There are four components to the postprocessor. The most important component is the suite of turbulence products. These include winds, streamlines, Richardson numbers, turbulence kinetic energy, and four turbulence prediction indices. They are depicted on horizontal surfaces from 16,000 feet to 46,000 feet in 2,000-foot intervals, as mid-upper tropospheric turbulence is the focus of the B-757 turbulence research flights.

The four turbulence potential predictive indices are as follows: Index #1 is the NASA Langley turbulence index that is primarily designed to determine layers of neutral static stability. Index #2 is based on the inertial instability parameter from Knox (1997). According to Knox (1997), it should be useful in cases of strong anticyclonic shear juxtaposed with low Richardson number indicative of environments favorable for clear-air turbulence (CAT). Index #3 is the NCSU1 index. NCSU1 is designed to be sensitive to inertial-advective forcing indicative of highly curved and accelerative jet stream flows. Finally, the index that we will demonstrate in section 3 is the NCSU2 index. This index, which was described in Kaplan et al. 2002, represents the cross product of the Montgomery stream function gradient and absolute vertical vorticity gradient on an isentropic surface passing through the specific height surface. It represents our most versatile and fundamental index that is designed to be applied to all three types of turbulence, i.e., CAT, convectively-induced turbulence (CIT), and mountain. It is based on the concept that along-stream ageostrophically-forced frontogenesis is favored during unbalanced supergradient wind flow regimes.

As ageostrophically-forced fronts form in confluent curved flows the along-stream gradient of temperature and relative vertical vorticity become superimposed as the geostrophic vertical vorticity maximum and total relative vertical vorticity maximum become displaced in space. Hence, a folded isentrope represents a region of convergence of along-stream-oriented maxima of vertical vorticity. The cross product of the pressure gradient and vorticity gradient maximizes where the pressure gradient force and gradients of vorticity maxima become orthogonal in contrast to geostrophic flow where the pressure gradient force and vorticity gradients are parallel.

The second most important component of the postprocessor is the convective products. As indicated by the results presented in Kaplan et al. 2002, CIT is a very common form of severe turbulence. Furthermore, the fundamental goal of the NASA B-757 research flights is to collect data for the certification of onboard turbulence-detecting radars. Hence, it is very important to be able to forecast regions of convection and convectively-induced turbulence potential. The products include: convective precipitation, total precipitation, cloud heights and cloud mass fluxes as diagnosed from the Kain-Fritsch (1990) convective parameterization scheme, the lifted index, and the k-index for all three grids.

The final two components of the product suite include skew-T/log-p soundings and accompanying convective forecasting parameters at all rawinsonde and most aviation surface station locations within each of the three grid matrix regions. In addition, vertical Froude number profiles are included at select locations along the Colorado Front Range of the Rocky Mountains for the coarse mesh grid only.

The temporal frequency of the turbulence, convective, sounding, and Froude number products is as follows:

- coarse mesh – turbulence, sounding, and Froude number products at initial time and every three hours; convective products at initial time plus three hours and every three hours thereafter
- fine1 mesh - the same except starting at three hours after 0000 UTC and 1200 UTC for turbulence and sounding products; convective products starting six hours after 0000 UTC and 1200 UTC
- fine2 mesh – the same for turbulence and sounding products except starting at six hours after 0000 UTC and 1200 UTC and every 90 minutes; convective products starting at 7.5 hours after 0000 UTC and 1200 UTC and every 90 minutes.

All horizontal plot products are available ~5 hours after observed data time for the coarse mesh, ~6 hours for the fine1 mesh, and ~7 hours for the fine2 mesh with sounding and Froude number products delayed ~2 hours after the horizontal plots for each grid. The computing is performed on a DEC-ALPHA workstation at the Department of Marine, Earth, and Atmospheric Sciences at North Carolina State University. All of these products are displayed at the following web site: http://shear.meas.ncsu.edu/

3. CASE STUDY EXAMPLES OF RTTM SIMULATIONS

In this section of the paper we will compare some of the RTTM products to the turbulence pilot reports (pireps), observations of winds, temperatures, and clouds, and the NCAR RAP ITFA turbulence potential forecast for a case study of widespread moderate turbulence (Sharman et al. 2000). This case study was simulated in real time with the RTTM. Most RTTM-simulated case studies of moderate or greater turbulence are associated with convective precipitation and jet entrance regions consistent with the findings in Kaplan et al. (2002).

The case study, 5 October 2001, strongly suggests that major differences exist when comparing the ITFA to the RTTM-generated NCSU2 index. These differences are likely the result of the development of a convective outflow jetlet. Figure 1 depicts the ITFA index at 30,000 feet and 1200 UTC 10/5/01. The high probability of turbulence is far to the north over Minnesota, Wisconsin, and the Upper Peninsula of Michigan in ITFA. However, the turbulence pireps during the ~1100 UTC – 1300 UTC time period depicted in Figure 2 indicate a swath of almost unbroken activity from Kansas through Missouri, Illinois, Indiana, and Ohio. This belt of observed turbulence lies well southeast of the ITFA maximum and is nearly coincident with the split structure in the convection in the water vapor imagery depicted in Figure 2b. Furthermore, the turbulence is closely aligned, actually just northwest of, the anticyclonic turning flow in the rawinsonde soundings at 1200 UTC superimposed on the RUC 200 mb winds depicted in Figure 2c. The rawinsonde sounding at Columbus, Ohio (ILN) at 1200 UTC (Fig. 3) indicated a deep neutral layer just above 450 mb and extending through ~350 mb near a shallow wind maximum. Hence, there is some proof supporting an observed convectively-enhanced jetlet that acts to split the flow and produce conditions favorable for turbulence as noted in Kaplan et al. (2002).

The 90-minute convective precipitation as well as 36,000-foot winds and 30,000-foot NCSU2 index values valid at 1200 UTC 10/5/01 from the 0000 UTC 10/5/01 RTTM fine2 simulation are depicted in Figures 4a-c. These figures show how the RTTM is developing a separate and deep convectively-enhanced anticyclonic outflow jetlet from southeastern Missouri to northern Ohio south of the main jet's entrance region producing a swath of high turbulence probability near the observed turbulence and well southeast of the ITFA maximum. The heavy convective precipitation, that is simulated to occur over Missouri in the RTTM fine2 product, results in latent heating-induced height rises that act to

accelerate the flow downstream over northern Illinois, Indiana, and Ohio. The accelerative flow provides the ageostrophic vertical vorticity gradients necessary to trigger large NCSU2 index values south of the large-scale jet entrance region and close to the observed turbulence. The lack of such a signal in ITFA indicates a likely underprediction of convective precipitation and/or a limitation of the physics in the index.

4. SUMMARY AND CONCLUSIONS

This paper has described a Real-Time Turbulence Model, its postprocessor, and an example of its ability to isolate regions of turbulence potential resulting from convectively-induced outflow jetlets.
The real-time system supports the NASA B-757 turbulence research missions and its products are available at: http://shear.meas.ncsu.edu/

Acknowledgements

This research has been funded under NASA contract #NAS1-99074 and subcontract #82U-7473-008 from the Research Triangle Institute. The authors wish to acknowledge the support of Dr. Fred H. Proctor, the NASA-Langley technical contract monitor and Neil J. O'Connor, the NASA Langley Turbulence Program manager.

References

Kain, J. S., and J. M. Fritsch, 1990: A one-dimensional entraining/detraining plume model. J. Atmos. Sci., 47, 2784-2802.

Kaplan, M. L., A. W. Huffman, K. M. Lux, J. D. Cetola, J. J. Charney, A. J. Riordan, Y.-L. Lin, and K. T. Waight III, 2002: Characterizing the severe turbulence environments associated with commercial aviation accidents. Part II: Hydrostatic mesoscale numerical simulations of supergradient wind flow and ageostrophic along-stream frontogenesis. Submitted, J. Appl. Meteor.

Knox, J. A., 1997: Possible mechanisms of clear air turbulence in strongly anticyclonic flows. Mon. Wea. Rev., 125, 1251-1259.

Sharman, R. G. Wiener, and B. Brown, 2000: Description and verification of the NCAR Integrated Turbulence Forecasting Algorithm (ITFA). AIAA 00-0493. AIAA 38th Aerospace Sciences Meeting and Exhibit, 10-13 January 2000, AIAA, Reno, NV.

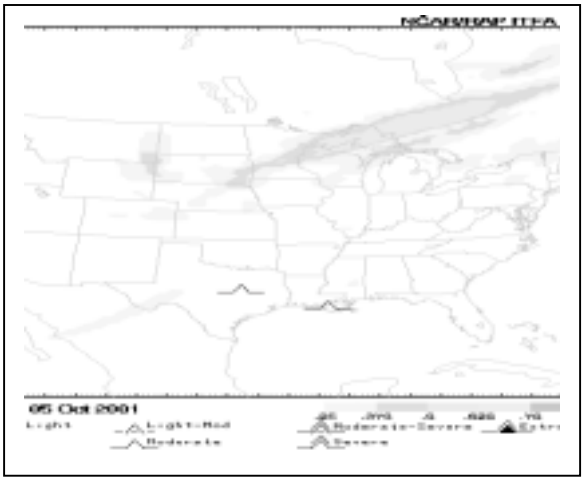

Figure 1. The ITFA index valid at 30,000 feet and 1200 UTC 5 October 2001.

Figure 2a. Pireps (heights in hundreds of feet) valid from 1126 UTC – 1320 UTC 5 October 2001.

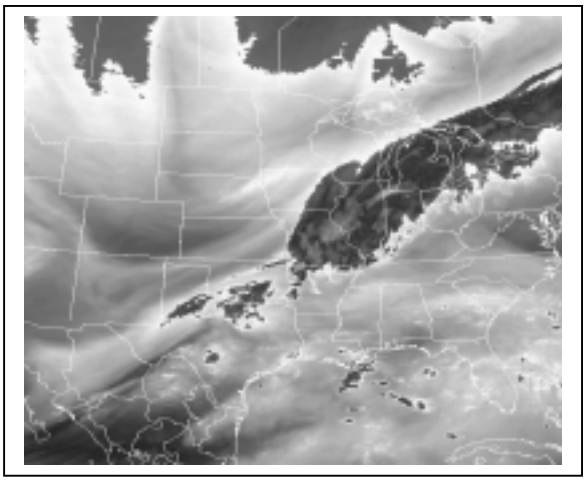

Figure 2b. Water vapor infrared satellite imagery valid at 1315 UTC 5 October 2001.

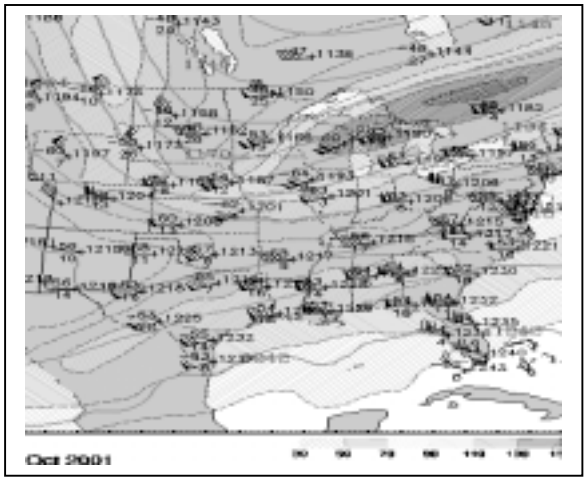

Figure 2c. 200 mb winds (knots) and heights (m) from the operational RUC model valid at 1500 UTC and superimposed 1200 UTC rawinsonde observations for 5 October 2001.

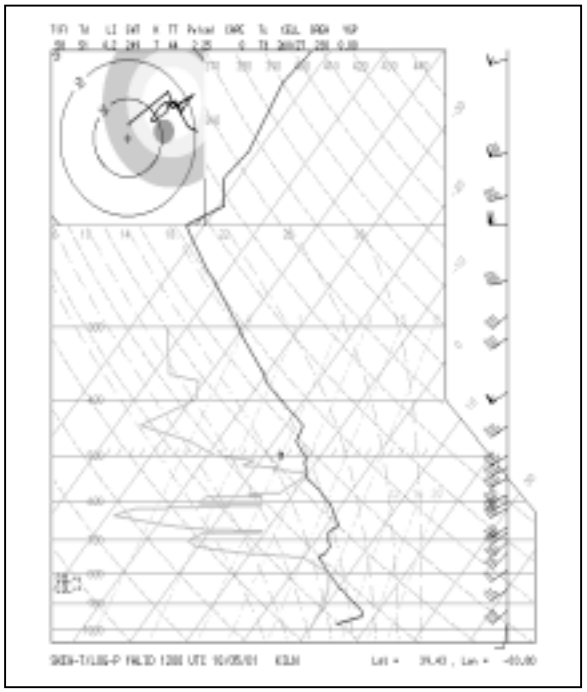

Figure 3. Columbus, Ohio (ILN) rawinsonde-derived sounding valid at 1200 UTC 5 October 2001.

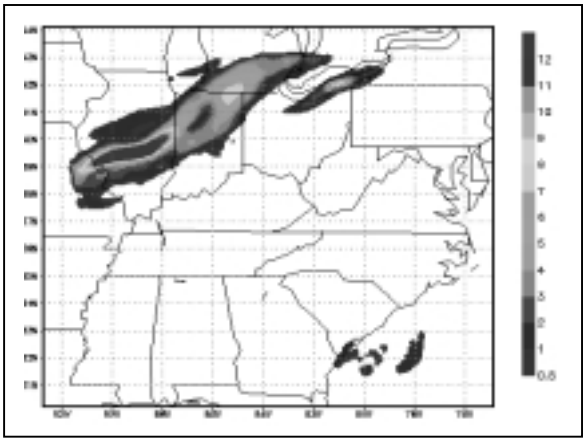

Figure 4a. RTTM fine2 90-minute precipitation (mm) valid from 1030 UTC – 1200 UTC 5 October 2001.

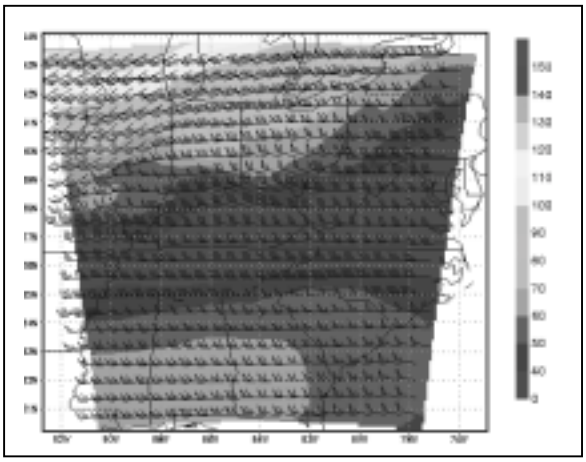

Figure 4b. RTTM fine2 wind vectors and isotachs (knots) valid at 36,000 feet and 1200 UTC 5 October 2001.

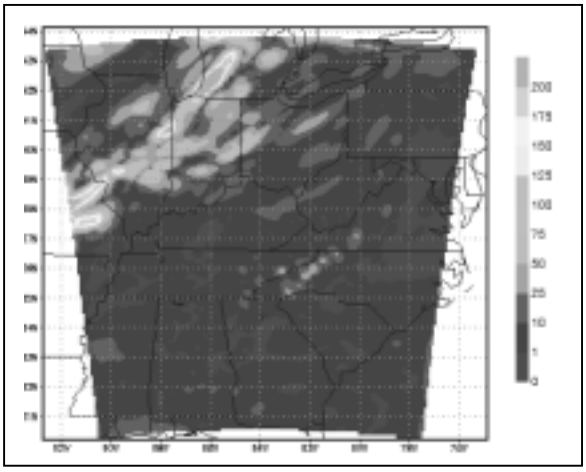

Figure 4c. RTTM fine2 NCSU2 index (x 10-12 s-3) valid at 30,000 feet and 1200 UTC 5 October 2001.